CrossMark

Observations of Heating along Intermittent Structures in the Inner Heliosphere from *PSP* Data

R. A. Qudsi[1], B. A. Maruca[2], W. H. Matthaeus[2], T. N. Parashar[1], Riddhi Bandyopadhyay[1], R. Chhiber[1,2],
A. Chasapis[3], Melvyn L. Goldstein[4,5], S. D. Bale[6,7,8], J. W. Bonnell[6], T. Dudok de Wit[9], K. Goetz[10], P. R. Harvey[6],
R. J. MacDowall[11], D. Malaspina[3], M. Pulupa[6], J. C. Kasper[12,13], K. E. Korreck[13], A. W. Case[13], M. Stevens[13],
P. Whittlesey[6], D. Larson[6], R. Livi[6], M. Velli[14], and N. Raouafi[15]

[1] Department of Physics and Astronomy, University of Delaware, Newark, DE 19716, USA
[2] Department of Physics and Astronomy, Bartol Research Institute, University of Delaware, Newark, DE 19716, USA
[3] Laboratory for Atmospheric and Space Physics, University of Colorado Boulder, Boulder, CO 80303, USA
[4] NASA Goddard Space Flight Center, Greenbelt, MD 20771, USA
[5] University of Maryland Baltimore County, Baltimore, MD 21250, USA
[6] Space Sciences Laboratory, University of California, Berkeley, CA 94720-7450, USA
[7] Physics Department, University of California, Berkeley, CA 94720-7300, USA
[8] The Blackett Laboratory, Imperial College London, London, SW7 2AZ, UK
[9] LPC2E, CNRS and University of Orléans, Orléans, France
[10] School of Physics and Astronomy, University of Minnesota, Minneapolis, MN 55455, USA
[11] Code 695, NASA Goddard Space Flight Center, Greenbelt, MD 20771, USA
[12] Climate and Space Sciences and Engineering, University of Michigan, Ann Arbor, MI 48109, USA
[13] Smithsonian Astrophysical Observatory, Cambridge, MA 02138 USA
[14] Department of Earth, Planetary, and Space Sciences, University of California, Los Angeles, CA 90095, USA
[15] Johns Hopkins University Applied Physics Laboratory, Laurel, MD, USA

Abstract

The solar wind proton temperature at 1 au has been found to be correlated with small-scale intermittent magnetic structures, i.e., regions with enhanced temperature are associated with coherent structures, such as current sheets. Using *Parker Solar Probe* data from the first encounter, we study this association using measurements of the radial proton temperature, employing the partial variance of increments (PVI) technique to identify intermittent magnetic structures. We observe that the probability density functions of high PVI events have higher median temperatures than those with lower PVI. The regions in space where PVI peaks were also locations that had enhanced temperatures when compared with similar regions, suggesting a heating mechanism in the young solar wind that is associated with intermittency developed by a nonlinear turbulent cascade in the immediate vicinity.

1. Introduction

Solar wind is a stream of charged particles emanating from Sun, originating in the corona (Parker 1960, 1963). It is highly magnetized collisionless plasma streaming at supersonic speeds and is primarily composed of ionized hydrogen (i.e., protons; Marsch et al. 1982; Kasper et al. 2012).

Despite decades of observation, the exact process that originally heats and accelerates solar wind plasma remains unknown, but several candidates have been proposed. Turbulence cascade transfers energy from large to small scales, which can ultimately lead to dissipation and heating (Velli et al. 1989; Velli 1993; Matthaeus et al. 1999; Dmitruk et al. 2002; Cranmer & van Ballegooijen 2005; Cranmer et al. 2007; Verdini & Velli 2007; Chandran & Hollweg 2009; Verdini et al. 2009a, 2009b; Cranmer 2012; Perez & Chandran 2013; Cranmer 2014; Lionello et al. 2014). Current sheets, generated by cascading vortices, can also lead to localized heating (Parashar et al. 2009; Osman et al. 2011, 2012a, 2012b; Gingell et al. 2015). Wave particle interactions—including, e.g., microinstabilities, Landau damping, and ion-cyclotron resonance—can likewise result in heating and other dramatic changes to the particles' phase-space distribution (Gary 1993; Sahraoui et al. 2010; Klein & Howes 2015).

In this study, we focused on coherent structures: features in the plasma that are persistent through time, concentrated in space, or both (Greco et al. 2018). Such structures can be produced by turbulent cascade (Osman et al. 2012b) and are also associated with current sheets (Yordanova et al. 2016). Osman et al. (2011, 2012b) analyzed in situ observations of near-Earth solar wind and found clear indications that coherent structures correlate with local enhancements in temperature.

In this study, we revisit the techniques of Osman et al. (2011, 2012b), and, by applying them to observations from the *Parker Solar Probe* (*PSP*), explore the relationship between plasma structures and heating in nascent solar wind plasma. Section 2 provides the background on such structures and introduces the reader to the physics of the technique employed in the data analysis, which is described in Section 3. In Section 4, we present the results and discuss its implication. Section 5 summarizes the results along with a conclusion and potential future works.

2. Background

The solar wind at 1 au exhibits localized structures that have been studied since the pioneering work of Burlaga (1968), Hudson (1970), Tsurutani & Smith (1979), and others and more recently by Ness & Burlaga (2001), Neugebauer (2006), and ErdőS & Balogh (2008). Several studies have found evidence that plasma turbulence generates these structures dynamically (Matthaeus & Lamkin 1986; Veltri 1999; Osman

et al. 2013). The structures are inhomogeneous and highly intermittent (Greco et al. 2008; Osman et al. 2011, 2013).

Some recent studies, both observational and numerical, have shown that these structures are correlated with the regions of enhanced temperature in the plasma (Osman et al. 2011, 2012a; Greco et al. 2012), and understanding the mechanisms by which the turbulence heats the plasma may also help solve the coronal heating problem (Osman et al. 2012b). This is a particularly attractive scenario, especially given the ubiquity of the localized structures. Study performed on data from the Particle in Cell (PIC) simulation by Wu et al. (2013) shows that the correlation between enhanced temperature and coherent structures exists for sub-ion inertial length (d_i). Further evidence of this is provided by TenBarge & Howes (2013) for the Gyrokinetic simulation; by Parashar et al. (2009), Wan et al. (2012, 2015), and Karimabadi et al. (2013) for the PIC simulation, and Servidio et al. (2012, 2015) for the Vlasov simulations, respectively. Work done by Chasapis et al. (2015) and Yordanova et al. (2016) employing Cluster and Magnetospheric Multiscale Mission (MMS) data show similar results from an observational vantage point.

In this study, we investigate these discontinuities in the magnetic field and explore their association with local enhancements in the ion temperature. One method for identifying a discontinuity in a time series of magnetic field (or any other) data is the partial variance of increments (PVI) methods, which is both a powerful and reliable tool for identifying and locating such regions. Following Greco et al. (2008), we define normalized PVI as

$$\mathcal{I}(t, \Delta t) = \frac{|\Delta \boldsymbol{B}(t, \Delta t)|}{\sqrt{\langle |\Delta \boldsymbol{B}(t, \Delta t)|^2 \rangle}}, \qquad (1)$$

where $\Delta \boldsymbol{B}(t, \Delta t) = \boldsymbol{B}(t + \Delta t) - \boldsymbol{B}(t)$ is the vector increment in the magnetic field at any given time, t, and at a time lag of Δt. When studying local structures induced by turbulence, Δt is typically chosen to be, assuming the validity of Taylor's hypothesis (Taylor 1938), of the order of d_i. $\langle ... \rangle$ is the ensemble average over a period of time, and $\mathcal{I}$ is the normalized PVI. Osman et al. (2012b) showed that PVI values greater than 2.4 indicate the existence of strong non-Gaussian coherent structures. Although they constitute only a small fraction of the total data set, their contribution to the total internal energy per unit volume is great. This emphasizes the importance of using the PVI technique for such studies. We also note that an analogous examination of the association of PVI events with energetic particles was carried out at 1 au (Tessein et al. 2016). A corresponding study of the first *PSP* orbit using IS⊙IS data is reported by Bandyopadhyay et al. (2020).

3. Data Selection and Methodology

We analyzed data from *PSP*'s first encounter with the Sun (2018 October 31–November 11). The FIELDS fluxgate magnetometers provided measurements of the local magnetic field at a rate of 64 samples/NYseconds, where 1 NYsecond is approximately 0.837 s (for an exact definition, see Bale et al. 2016). Radial proton temperature/thermal speed data were obtained from the Solar Probe Cup (SPC), which is a part of the Solar Wind Electron, Alpha and Proton (SWEAP) suite (Kasper et al. 2016). The average speed of solar wind during the first encounter was around 350 km s^{-1} for the most part and
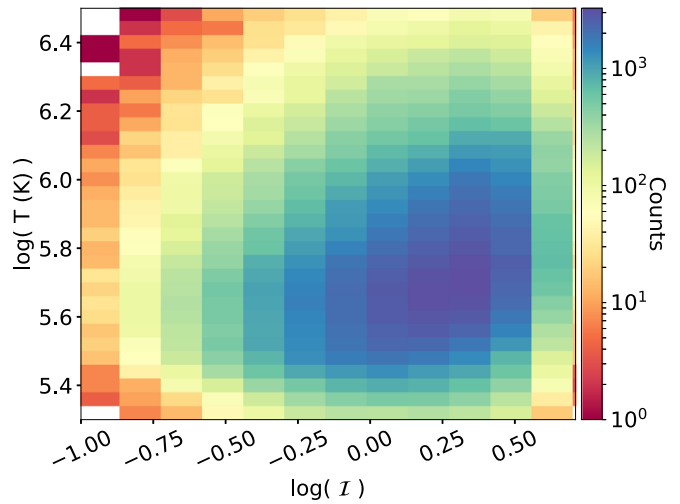

Figure 1. Joint histogram of the radial proton temperature and PVI for the second half of the first encounter on a log–log scale. There is an upward trend between PVI and the temperature as the blue region in the plot tilts upward, showing an increase in the temperature as PVI increases.

crossed 500 km s^{-1} only on the last day of the encounter. Thus, using Taylor's hypothesis, 1 NYs corresponds to a length scale of 300 km.

Since SPC only measures the radial temperature, and the proton temperature is expected to be significantly anisotropic, we needed to ensure that the temperature we were measuring was indeed the parallel temperature. Thus, we only considered data points where magnetic field was mostly radial. Any interval where the angle between $B_r \hat{\boldsymbol{r}}$ and $\boldsymbol{B}$ was more than 30° was not considered. This ensured that the temperature measured by SPC was indeed the parallel temperature. For the calculation of PVI according to Equation (1), we used 64 NYHz data, with a lag of 1 NYs, which is the native cadence of SPC (Kasper et al. 2016). The ensemble averaging was done over 8 hr, which is several times the estimated correlation time. In this study, we used the correlation time computed in Parashar et al. (2020). However, there are a few subtleties associated with this calculation, and Smith et al. (2001), Isaacs et al. (2015), Krishna Jagarlamudi et al. (2019), and Bandyopadhyay et al. (2020) offer more insights and discussion on this topic along with potential issues in such determination. We also carried out the analysis for various different averaging times (from 1 to 12 hr) and it was observed to have minimal affect on the outcome. The PVI time series was then resampled to an ion cadence of 1NYHz in the way such that for each interval of 1 NYs, the maximum value of PVI in that interval was chosen.

In this study, we focused on the second half of the encounter immediately after *PSP* was at its perihelion. The second half of the encounter has very different properties compared to the first half. A greater number of energetic particles were observed (McComas et al. 2019), the solar wind speed was higher (Kasper et al. 2019), and there were many more switchbacks (Bale et al. 2019). Bandyopadhyay et al. (2020) observed enhanced local energy transfer, which points toward a more turbulent period in general, and thus a suitable environment for PVI study.
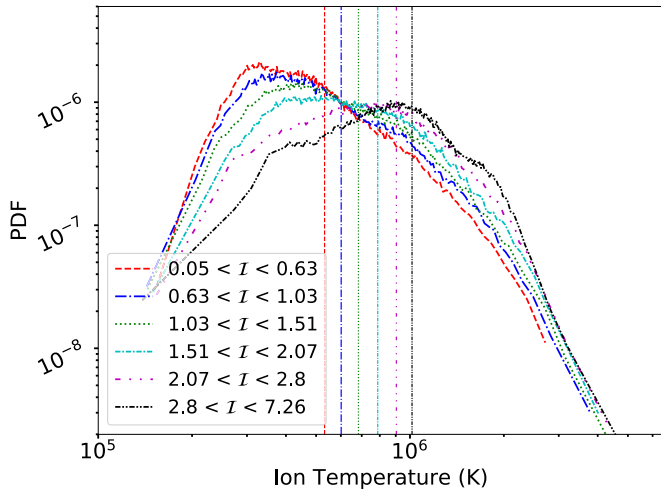
Figure 2. Probability distribution functions(PDFs) for the radial proton temperature for the second half of the first encounter. Each PDF corresponds to a different PVI range such that each PVI bin has an equal number of data points. The probability density increases with the increase in temperature for high PVI, whereas it decreases for a low PVI PDF. Vertical lines show the median temperature for each of the PDF plots.

4. Results and Discussion

Figure 1 shows the joint histogram of the radial proton temperature and PVI for the first encounter. Increasing PVI color contours have an upward trend, as we see the temperature distribution showing a positive slope with an increase in the value of PVI. The positive correlation between the temperature and PVI suggest some kind of heating in the regions with high PVI. We then conditionally sampled the radial proton temperature. Conditionally sampling means that we arrange the data by an increasing value of PVI and then divide all the data points in 6 bins such that each bin has equal number of points. We then calculate the temperature distribution within each bin, which is shown in Figure 2.

As PVI increases, the probability density increases for the higher temperature and decreases for the lower temperature, which is opposite of what we see at the low temperatures where the probability density is highest for the lowest PVI. The median temperature, shown by vertical lines in Figure 2, for each of the distribution increases, implying the presence of stronger and stronger heating as we go to higher and more extreme values of PVI. For PVI < 1, the median value of the temperature is 5.32×10^5 K, whereas for PVI > 6, the median temperature increases to 1.01×10^6 K. Osman et al. (2011) observed a similar increase in the average temperature in their study of solar wind at 1 au. This is consistent with heating occurring in the regions with a small-scale coherent structure in magnetohydrodynamic turbulence.

In order to further demonstrate this relationship, we looked at the temperature at the point of the high PVI event and its immediate surrounding in space using the methodology described by Osman et al. (2012b). We compute the mean value of the temperature at the point of the PVI event and for points near the PVI events separated from it by up to one correlation length. Formally, these averages may be expressed as

$$\widetilde{T}_p(\Delta t, \theta_1, \theta_2) = \langle T_p(t_{\mathcal{I}} + \Delta t) | \theta_1 \leqslant \mathcal{I}(t_{\mathcal{I}}) < \theta_2 \rangle, \qquad (2)$$
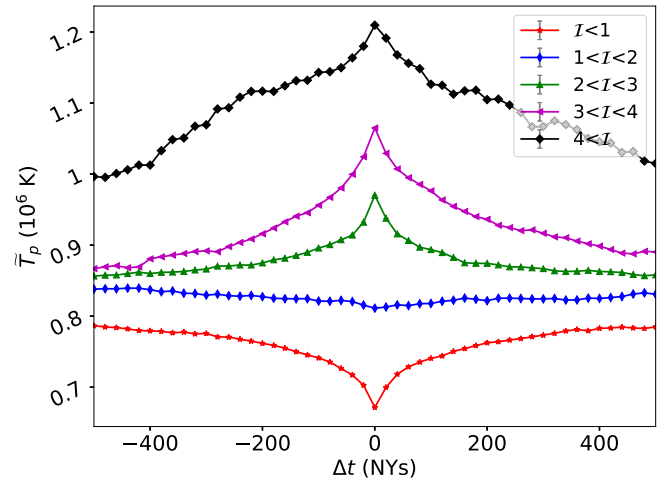

Figure 3. The plot shows the conditional average temperature for different PVI thresholds at the point of a PVI event. $\widetilde{T}_p$ peaks at the instant of PVI event and continues to have an elevated temperature in its vicinity within the correlation timescale. The red curve, corresponding to lowest PVI, shows a dip, suggesting no heating when the magnetic field is very smooth.

where $\widetilde{T}_p$ is the conditionally average temperature for all the events, Δt is the time difference relative to the position of PVI events, and $t_{\mathcal{I}}$ is the time of PVI events between the threshold θ_1 and θ_2.

Figure 3 shows the plot of $\widetilde{T}_p$ for various thresholds for the second half of the encounter. Not only do we observe an enhanced temperature at the point of high PVI events, suggesting localized heating at those points, but we also see that $\widetilde{T}_p$ a higher PVI event is consistently higher than nearby points separated by up to a correlation length. This implies that the points nearby an identified PVI event have an elevated average temperature, continuously approaching the elevated average temperature found at the PVI event itself. Some of this effect may be due to clustering of PVI events (see Chhiber et al. 2020). Another point worth noting in Figure 3 is the valley in the temperature profile for small PVI. This is the region where background magnetic field is smooth, and it appears that in such regions, the temperature is lower than the temperature of plasma in its immediate surrounding, which is concurrent with the fact that in those places, there is no turbulence heating. Osman et al. (2012b) found similar result in their study at 1 au. However, in our study, we find a significant dip compared to the dip reported in Osman et al. (2012b): $\sim 10^5$ K compared to $\sim 2 \times 10^5$ K.

5. Conclusion

In this study, we used in situ observations from *PSP*'s first encounter with the Sun to explore the association of proton heating with coherent magnetic structures in the young solar wind. We identified enhancements of PVI (Greco et al. 2008) as indications of the presence of such a structure (Osman et al. 2011, 2012b). We observed that the joint histogram of PVI and the proton radial temperature shows a positive trend as shown in Figure 1. We also observed that the PDF of data, as shown in Figure 2, with higher PVI has a higher mean temperature compared to those with lower PVI. This strongly supports the theory that the solar wind in those regions are heated by coherent structures, which are generated by plasma turbulence.

The present results demonstrate both the shifting of the PDF of the temperature toward higher values with the increasing

PVI condition (in Figure 2) and the spatial/temporal localization of the temperature enhancement near PVI events (in Figure 3). Both of these are fully consistent with findings in the two papers that examine these effects (Osman et al. 2011, 2012a), respectively, at 1 au. It is interesting that these effects are clearly present in the *PSP* first orbit where turbulence is presumably younger and possibly less well developed than it is at 1 au. It is possible that the temperature differential between low and high PVI is somewhat less in the *PSP* data than in the *ACE* data at 1 au (Osman et al. 2011), but additional samples by *PSP* will be needed to draw any firm conclusion of this type.

In order to further demonstrate this association, we looked at the conditionally average temperatures at the point of a high PVI event and in its immediate surrounding up to 1 correlation length. We observed that not only does the point of event has the highest temperature, but its vicinity shows enhanced temperatures compared to lower PVI events. The local maxima of these temperature profiles are most prominent from higher PVI events, suggesting stronger heating. The plateau regions of each thresholds are distinct, and for higher threshold, they maintain a high value, suggesting clustering of PVI events around a large discontinuity. For a very smooth magnetic field, we see a dip in the average temperature at that point. Osman et al. (2012b) found similar behavior in their study of solar wind at 1 au, though neither the heating nor the dip in the temperature for small PVI that they reported in their study was as high as what we observed in our study. This suggests that either coherent structures are more efficient in heating the plasma near the Sun compared to 1 au or that we have more such structures as we move closer to the Sun. Since these coherent structures are generated by plasma turbulence, these observations suggest that nonlinear turbulence cascades play a crucial role in heating the nascent solar wind. Given the ubiquitous nature of such structures, this process can help explain the coronal heating.

A significant limitation of this study was the unavailability of temperature anisotropy data. The temperature measures we used were not the scalar temperature but rather the radial temperature, for which reason we limited our observations to the period of the nearly radial magnetic field (see Section 3). Once ion temperature anisotropy data are available, we will revisit this work to explore both scalar and anisotropic heating. Theoretical studies have found that turbulent cascade can generate strong temperature anisotropy near coherent structures (Parashar & Matthaeus 2016).

We also hope to further explore Figure 3. Careful inspection of this plot reveals a very slight asymmetry in the shape of the temperature profile before and after the PVI event. The phenomenon was also noted in 1 au solar wind by Osman et al. (2012b). The cause and significance of this asymmetry remain unclear, but it may suggest a connection between local heating and large-scale processes, such as a heat flux.

ORCID iDs

R. A. Qudsi https://orcid.org/0000-0001-8358-0482
B. A. Maruca https://orcid.org/0000-0002-2229-5618
W. H. Matthaeus https://orcid.org/0000-0001-7224-6024
T. N. Parashar https://orcid.org/0000-0003-0602-8381
Riddhi Bandyopadhyay https://orcid.org/0000-0002-6962-0959
R. Chhiber https://orcid.org/0000-0002-7174-6948
A. Chasapis https://orcid.org/0000-0001-8478-5797
Melvyn L. Goldstein https://orcid.org/0000-0002-5317-988X
S. D. Bale https://orcid.org/0000-0002-1989-3596
P. R. Harvey https://orcid.org/0000-0002-6938-0166
R. J. MacDowall https://orcid.org/0000-0003-3112-4201
D. Malaspina https://orcid.org/0000-0003-1191-1558
M. Pulupa https://orcid.org/0000-0002-1573-7457
J. C. Kasper https://orcid.org/0000-0002-7077-930X
K. E. Korreck https://orcid.org/0000-0001-6095-2490
A. W. Case https://orcid.org/0000-0002-3520-4041
M. Stevens https://orcid.org/0000-0002-7728-0085
P. Whittlesey https://orcid.org/0000-0002-7287-5098
M. Velli https://orcid.org/0000-0002-2381-3106

References

Bale, S. D., Goetz, K., Harvey, P. R., et al. 2016, SSRv, 204, 49
Bale, S., Badman, S. T., & Bonnell, J. W. 2019, Natur, 576, 237
Bandyopadhyay, R., Matthaeus, W. H., Parashar, T. N., et al. 2020, ApJS, doi:10.3847/1538-4365/ab6220
Burlaga, L. F. 1968, SoPh, 4, 67
Chandran, B. D. G., & Hollweg, J. V. 2009, ApJ, 707, 1659
Chasapis, A., Retinò, A., Sahraoui, F., et al. 2015, ApJL, 804, L1
Chhiber, R., Goldstein, M. L., Maruca, B. A., et al. 2020, ApJS, doi:10.3847/1538-4365/ab53d2
Cranmer, S. R. 2012, ApJ, 754, 92
Cranmer, S. R. 2014, ApJS, 213, 16
Cranmer, S. R., & van Ballegooijen, A. A. 2005, ApJS, 156, 265
Cranmer, S. R., van Ballegooijen, A. A., & Edgar, R. J. 2007, ApJS, 171, 520
Dmitruk, P., Matthaeus, W. H., Milano, L. J., et al. 2002, ApJ, 575, 571
Erdős, G., & Balogh, A. 2008, AdSpR, 41, 287
Gary, S. P. 1993, Theory of Space Plasma Microinstabilities (Cambridge: Cambridge Univ. Press)
Gingell, P. W., Burgess, D., & Matteini, L. 2015, ApJ, 802, 4
Greco, A., Chuychai, P., Matthaeus, W. H., Servidio, S., & Dmitruk, P. 2008, GeoRL, 35, L19111
Greco, A., Matthaeus, W. H., Perri, S., et al. 2018, SSRv, 214, 1
Greco, A., Valentini, F., Servidio, S., & Matthaeus, W. H. 2012, PhRvE, 86, 066405
Hudson, P. 1970, P&SS, 18, 1611
Isaacs, J. J., Tessein, J. A., & Matthaeus, W. H. 2015, JGRA, 120, 868
Karimabadi, H., Roytershteyn, V., Wan, M., et al. 2013, PhPl, 20, 012303
Kasper, J. C., Abiad, R., Austin, G., et al. 2016, SSRv, 204, 131
Kasper, J. C., Stevens, M. L., Korreck, K. E., et al. 2012, ApJ, 745, 162
Kasper, J. C., Bale, S. D., & Belcher, J. W. 2019, Natur, 576, 228
Klein, K. G., & Howes, G. G. 2015, PhPl, 22, 032903
Krishna Jagarlamudi, V., Dudok de Wit, T., Krasnoselskikh, V., & Maksimovic, M. 2019, ApJ, 871, 68
Lionello, R., Velli, M., Downs, C., et al. 2014, ApJ, 784, 120
Marsch, E., Mühlhäuser, K.-H., Rosenbauer, H., Schwenn, R., & Neubauer, F. M. 1982, JGR, 87, 35
Matthaeus, W. H., & Lamkin, S. L. 1986, PhFl, 29, 2513
Matthaeus, W. H., Zank, G. P., Oughton, S., Mullan, D. J., & Dmitruk, P. 1999, ApJL, 523, L93
McComas, D. J., Christian, E. R., Cohen, C. M. S., et al. 2019, Natur, 576, 223
Ness, N. F., & Burlaga, L. F. 2001, JGRA, 106, 15803
Neugebauer, M. 2006, JGRA, 111, A04103
Osman, K. T., Matthaeus, W. H., Greco, A., & Servidio, S. 2011, ApJL, 727, L11
Osman, K. T., Matthaeus, W. H., Hnat, B., & Chapman, S. C. 2012a, PhRvL, 108, 261103

Osman, K. T., Matthaeus, W. H., Kiyani, K. H., Hnat, B., & Chapman, S. C. 2013, PhRvL, 111, 201101

Osman, K. T., Matthaeus, W. H., Wan, M., & Rappazzo, A. F. 2012b, PhRvL, 108, 261102

Parashar, T. N., Goldstein, M. L., Maruca, B. A., et al. 2020, ApJS, doi:10.3847/1538-4365/ab64e6

Parashar, T. N., & Matthaeus, W. H. 2016, ApJ, 832, 57

Parashar, T. N., Shay, M. A., Cassak, P. A., & Matthaeus, W. H. 2009, PhPl, 16, 032310

Parker, E. N. 1960, ApJ, 132, 821

Parker, E. N. 1963, Interplanetary Dynamical Processes (New York: Interscience Publishers)

Perez, J. C., & Chandran, B. D. G. 2013, ApJ, 776, 124

Sahraoui, F., Goldstein, M. L., Belmont, G., Canu, P., & Rezeau, L. 2010, PhRvL, 105, 131101

Servidio, S., Valentini, F., Califano, F., & Veltri, P. 2012, PhRvL, 108, 045001

Servidio, S., Valentini, F., Perrone, D., et al. 2015, JPlPh, 81, 325810107

Smith, C. W., Matthaeus, W. H., Zank, G. P., et al. 2001, JGR, 106, 8253

Taylor, G. I. 1938, RSPSA, 164, 476

TenBarge, J. M., & Howes, G. G. 2013, ApJL, 771, L27

Tessein, J. A., Ruffolo, D., Matthaeus, W. H., & Wan, M. 2016, GeoRL, 43, 3620

Tsurutani, B. T., & Smith, E. J. 1979, JGRA, 84, 2773

Velli, M. 1993, A&A, 270, 304

Velli, M., Grappin, R., & Mangeney, A. 1989, PhRvL, 63, 1807

Veltri, P. 1999, PPCF, 41, A787

Verdini, A., & Velli, M. 2007, ApJ, 662, 669

Verdini, A., Velli, M., & Buchlin, E. 2009a, ApJL, 700, L39

Verdini, A., Velli, M., Matthaeus, W. H., Oughton, S., & Dmitruk, P. 2009b, ApJL, 708, L116

Wan, M., Matthaeus, W. H., Karimabadi, H., et al. 2012, PhRvL, 109, 195001

Wan, M., Matthaeus, W. H., Roytershteyn, V., et al. 2015, PhRvL, 114, 175002

Wu, P., Perri, S., Osman, K., et al. 2013, ApJL, 763, L30

Yordanova, E., Vörös, Z., Varsani, A., et al. 2016, GeoRL, 43, 5969